Effect of Austempering on Plastic Behavior of some ADI Alloys

Jakob Olofsson*[1], Dan Larsson[1, 2] and Ingvar L Svensson[1]

[1] Jönköping University, School of Engineering, Dept Mechanical Engineering
Materials and Manufacturing – Casting
P.O. Box 1026, SE-551 11 Jönköping, Sweden
[2] Present affiliation: Vestascastings Guldsmedshyttan AB, SE-711 78, Guldsmedshyttan, Sweden
* Corresponding author, email jakob.olofsson@jth.hj.se

ABSTRACT

A numerical description relating microstructure to elastic and plastic deformation behavior would make it possible to simulate the mechanical behavior of complex cast components with tailored material properties. Limited work and data have however been published regarding the connection between microstructure and plastic behavior of austempered ductile irons (ADI). In the current work the effects of austempering temperature and austempering time on the strength coefficient and the strain hardening exponent of the Hollomon equation have been investigated for two ADI alloys. The results show that the plastic behavior is highly dependent on the combination of austempering temperature and austempering time. It was found that as the austempering temperature increases both the strength coefficient and the strain hardening exponent initially decrease, but after reaching a minimum at the critical austempering temperature they show a plateau or an increase. The effect of the austempering time on the plastic behavior depends on the austempering temperature. At low austempering temperatures the strength coefficient and the strain hardening exponent decrease with increased austempering time, whereas at higher austempering temperatures they show little time dependence. These relations are explained by the microstructural transformations that take place during the austempering heat treatment.

I. INTRODUCTION

The industrial application of austempered ductile iron, ADI, has grown in recent years. The material has a number of mechanical properties that makes it attractive for structural applications in transport such as automotive, heavy vehicles and many other industries. The material can be tailored to have properties such as high strength, high wear resistance, high fracture toughness and high fatigue strength[1-3].

ADI is an alloyed ductile iron which has been subjected to a two-step heat treatment process known as austempering. The first step is austenitizing. The ductile iron is heated to the austenitizing temperature for sufficient time to obtain a fully austenitic matrix saturated with carbon. The next step is austempering, during which the ductile iron is quenched to the austempering temperature and held there for a period of time, the austempering time, before cooling to room temperature. During austempering the fully austenitic matrix transforms into acicular ferrite and stabilized high carbon austenite, a matrix called ausferrite. This reaction, where austenite (γ) decomposes into ferrite (α) and high carbon austenite (γ_{HC}), is known as the first stage reaction [2], Eq. [1].

$$\gamma \rightarrow \alpha + \gamma_{HC} \quad [1]$$

The first stage reaction consists of two substeps. In the first substep ferrite nucleates and the entire matrix transforms into acicular ferrite and austenite with a low carbon content of about 1.2-1.6%. In the second substep ferrite grows instead of further nucleation, while the carbon diffuses into austenite and creates high carbon austenite with a carbon level of about 1.8-2.2% [4]. The low carbon austenite is metastable: metastable austenite may exist at room temperature, but when further cooled or stressed it may transform to martensite[4]. Martensite is a hard and brittle phase that causes e.g. machining problems, and strain

induced martensite strongly influences the mechanical properties of ADI materials[4, 5]. The austempering time must thus be long enough to ensure that high carbon austenite is obtained and the formation of martensite is avoided. If the austempering time is too long however the high carbon content austenite becomes saturated with carbon and decomposes into ferrite (α) and carbide (ε)[4]. This is known as the second stage reaction[2], Eq. [2].

$$\gamma_{HC} \rightarrow \alpha + \varepsilon \quad [2]$$

This microstructure contains carbide, which makes the material brittle. The parameters of the austempering process must thus be selected so that the second stage reaction is avoided during the manufacturing of ADI[6].

At the beginning of the austempering, the entire matrix is austenitized. Because carbon distribution after solidification is nonuniform, the austempering reaction is also nonuniform. This results in three different types of austenite that can be found in the casting after austempering[4]. The first type is called *unreacted metastable austenite*, which has not participated in the austempering process. Its carbon content is thus the same as during austenitizing, about 0.8-1.1%. The second type is called *reacted metastable austenite*. The carbon content of this austenite has increased to typically 1.2-1.6% during austempering, and is still metastable. The third type, *reacted stable austenite*, has reached the stable carbon content of about 1.8-2.2%. The only desirable type of austenite after austempering is the reacted stable austenite, because the metastable austenite types may transform into martensite when the material is cooled or stressed. The designation *retained austenite* includes all these three types of austenite[4]. The amount of unreacted metastable austenite decreases as the austempering time increases, because a larger fraction of austenite has been able to participate in the austempering process.

The mechanical properties of ADI are related to the ausferritic matrix. By correctly controlling the austempering heat treatment, the mechanical properties of the material can be tailored to promote e.g. high strength, high wear resistance or high fracture toughness[1-3, 7]. The mechanical properties studied in this paper are the tensile properties achieved from a standard tensile test. For ADI as well as many other metallic engineering materials a fairly linear elastic behavior can be identified at stress levels below the yield stress, followed by a non-linear plastic behavior at stress levels above the yield stress. The linear elastic behavior is described by Hooke's law, Eq. [3], while many other models are available for the non-linear plastic behavior. In this paper the plastic behavior has been described using the Hollomon equation, Eq. [4].

$$\sigma = E * \varepsilon_{el} \quad [3]$$

$$\sigma = K * {\varepsilon_{pl}}^{n} \quad [4]$$

Here σ is the true stress (Pa), E is the Young's modulus (Pa), ε_{el} is the true elastic strain (dimensionless), K is the strength coefficient (Pa), ε_{pl} is the true plastic strain and n is the strain hardening exponent, both dimensionless. Note that Eq. [3] only is valid for the elastic contribution, while Eq. [4] only is valid for the plastic contribution. Because the yield stress corresponding to no plastic strain is often hard to determine, a proof stress corresponding to a certain amount of plastic strain is commonly used. In the current work the 0.2% proof stress has been used to compare the elastic properties of the materials.

By combining Hooke's law with the Hollomon equation the total strain, ε_T, can be written as the sum of the elastic and plastic contributions as shown in Eq. [5].

$$\varepsilon_T = \varepsilon_{el} + \varepsilon_{pl} = \frac{\sigma}{E} + \frac{\sigma^{1/n}}{K^{1/n}} \quad [5]$$

The strength coefficient *K* gives an indication of the strength potential of the material, but must be evaluated in combination with the strain hardening exponent *n*, which defines the work hardening capacity of a material. The strain hardening exponent can be used to compare the machinability of materials, where a low value of the strain hardening exponent corresponds to a good machinability of the material[8]. The strain hardening exponent can be seen as a factor related to the number of dislocations and their entanglement in the metal[9]. The value of the strain hardening exponent ranges between 0 and 1, where *n* = 0 describes a perfectly plastic material where $\sigma = K$, and a value of *n* = 1 describes a linear deformation hardening material where $\sigma = K * \varepsilon_{pl}$. Typical values of the strain hardening exponent for the current ADI materials were found to be in the range *n = 0.05-0.3* which corresponds to shapes of the plastic behaviors as shown in Figure 1.

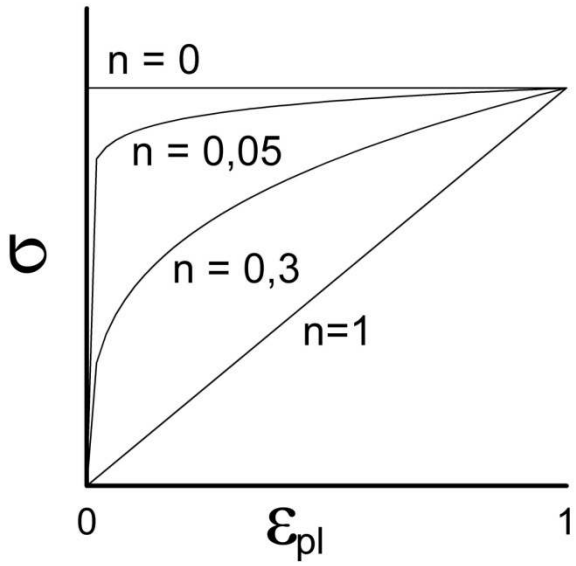

Figure 1: Effect of different values of the strain hardening exponent on the plastic behavior

Cast ADI components are often subjected to extensive machining operations. Previous research has shown a connection between the machinability of an ADI material and its strain hardening behavior[8]. A lower value of *n* implies a lower work hardening rate, which is preferred from a machining point of view. The ADI microstructure consists of, as described above, ferrite and austenite. Austenite has a higher work hardening rate than ferrite. Thus the machinability of the material will highly depend on the microstructure and the volume fraction of ferrite, both of which are dependent on the austempering heat treatment[10]. Much research has focused on the effect of austempering parameters on mechanical properties, but limited information is found in the literature concerning the relationship between the plastic behavior of ADI and the austempering parameters. Yang and Putatunda[8] commented on this lack of information but investigated only the relationship between austempering temperature and strain hardening exponent.

The objective of this study is to relate both austempering temperature and austempering time to both the strength coefficient *K* and the strain hardening exponent *n*, and explain these relations from a microstructural point of view. These relations need to be understood in order to create a numerical model that predicts machinability and total stress-strain behavior of ADI.

II. EXPERIMENTAL PROCEDURE

A. Materials

Two different but very similar ADI alloys have been investigated, here denoted ADI-1 and ADI-2. The as-cast materials were two alloyed ductile irons with chemical compositions according to Table I, cast during serial production of two ring components with an outer diameter of about 0.5 meter at two different foundries. These two alloys are very similar in chemical composition, and no major differences on the general behavior related to the chemical composition are expected. Cylindrical tensile specimens were prepared from the rings, with their long axis in the tangential direction. The tensile test specimens had a diameter of 7 mm, a gauge length of 50 mm and a total length of 98 mm. In total 40 specimens were prepared in ADI-1 and 64 specimens in ADI-2. Four test specimens of each material were used for testing the tensile properties of the as-cast materials and for microstructural analysis. The remaining test specimens were subjected to an austempering process. The austenitizing treatment was performed at 1173 K (900 °C) for 2 h, and the specimens were austempered at different temperatures and times as reported in Table II. For each combination of material, austempering temperature and austempering time three specimens were produced and tested. The results presented are the average values of these three samples. After metallographic preparation the austempered specimens were etched with 4% Nital solution and examined using optical microscopy.

Tensile tests were conducted at room temperature, using a Zwick/Roell Z100 testing machine with 100 kN load capacity and a cross-head speed of 0.5 mm/min. Stress-strain curves were obtained, from which the 0.2% proof strength, ultimate tensile strength and total strain were determined.

Table I. Chemical Composition of the Alloys

Wt. Pct	C	Si	Mn	P	S	Cr	Mo	Ni	Cu
ADI-1	3,46	2,25	0,37	0,02	0,006	0,04	0,20	0,03	0,78
ADI-2	3,65	2,13	0,34	0,03	0,009	0,04	0,27	0,05	0,82

Table II. Experimental Program; Austempering Temperatures and Times for the Materials

	Austempering times	
Austempering temperature	ADI-1	ADI-2
523 K (250 °C)	1h, 2h, 3h	0.5h, 1h, 2h, 3h
573 K (300 °C)	1h, 2h, 3h	0.5h, 1h, 2h, 3h
598 K (325 °C)	-	0.5h, 1h, 2h, 3h
623 K (350 °C)	1h, 2h, 3h	0.5h, 1h, 2h, 3h
673 K (400 °C)	1h, 2h, 3h	0.5h, 1h, 2h, 3h

B. Evaluation of Stress-strain Curves

The constants n and K in the Hollomon equation, Eq. [4], are determined by evaluating data from the tensile test curves. By plotting the curve using a double logarithmic plot of true stress against true plastic strain, a reasonably straight line is achieved where n is the slope and K is the stress level where ε_{pl} equals unity. This method has been implemented in Matlab in order to evaluate the parameters of the Hollomon equation directly from the stress-strain data obtained from the tensile tests. A comparison between the measured tensile curve and the curve described by combining Hooke's law and the Hollomon equation, Eq. [5], is shown in Figure 2.

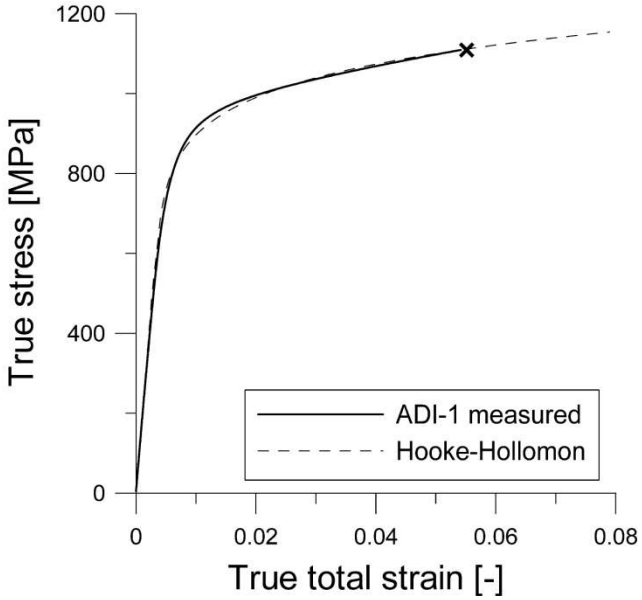

Figure 2: Comparison of measured tensile test curve and curve described by Hooke's law and the Hollomon equation for ADI-1 austempered at 350ºC for 2 hours

III. RESULTS AND DISCUSSION

A. Microstructure

Figure 3 and Figure 4 show examples of the microstructures of the two materials austempered at different temperatures and times. In the photomicrographs, graphite nodules are seen as dark circular areas dispersed in the matrix of ausferrite, consisting of bright austenite and dark acicular ferrite. During the austempering process ferrite plates form from the austenite. Ferrite dissolves very little carbon, thus for the ferrite needles to grow, carbon must diffuse from the ferrite into the surrounding austenite[8]. A low austempering temperature gives a larger undercooling of the austenite. This decreases the diffusion rate of carbon from ferrite into austenite, which favors nucleation of new ferrite plates in austenite rather than growth of the existing plates. Thus a finer ferrite structure is created at lower austempering temperatures[11], with a high volume fraction of ferrite and a low volume fraction of austenite[8]. With higher austempering temperatures the undercooling of the austenite decreases, which increases the carbon diffusion rate. This leads to decreased ferrite nucleation but increases the growth of existing ferrite plates. Thus a coarser ferrite structure is obtained[11] and the volume fraction of austenite increases[8] as illustrated in Figure 3 and Figure 4. The higher austempering temperature has resulted in a coarser ausferritic matrix with a higher fraction of austenite than the lower temperature.

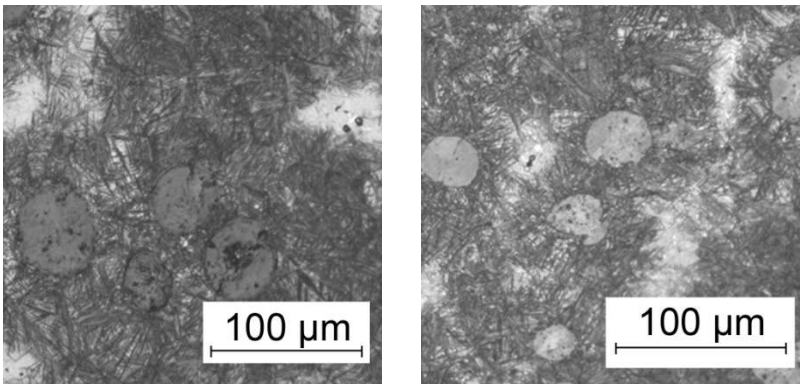

(a) *(b)*

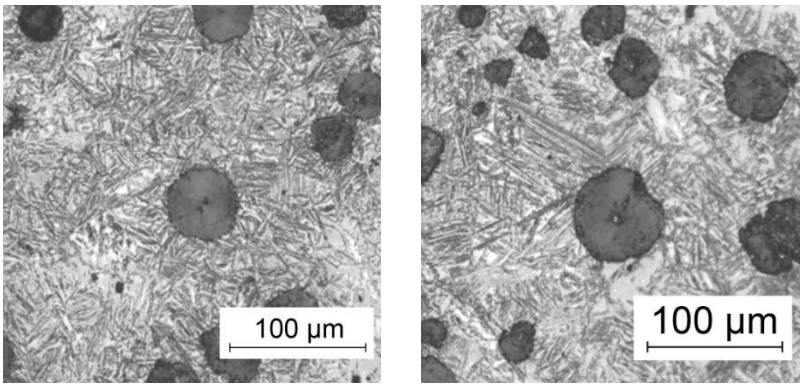

(c) *(d)*

Figure 3: Microstructure of ADI-1 austempered at 523 K (250 °C) for (a) 1 hour and (b) 3 hours, respectively 673 K (400 °C) for (c) 1 hour and (d) 3 hours

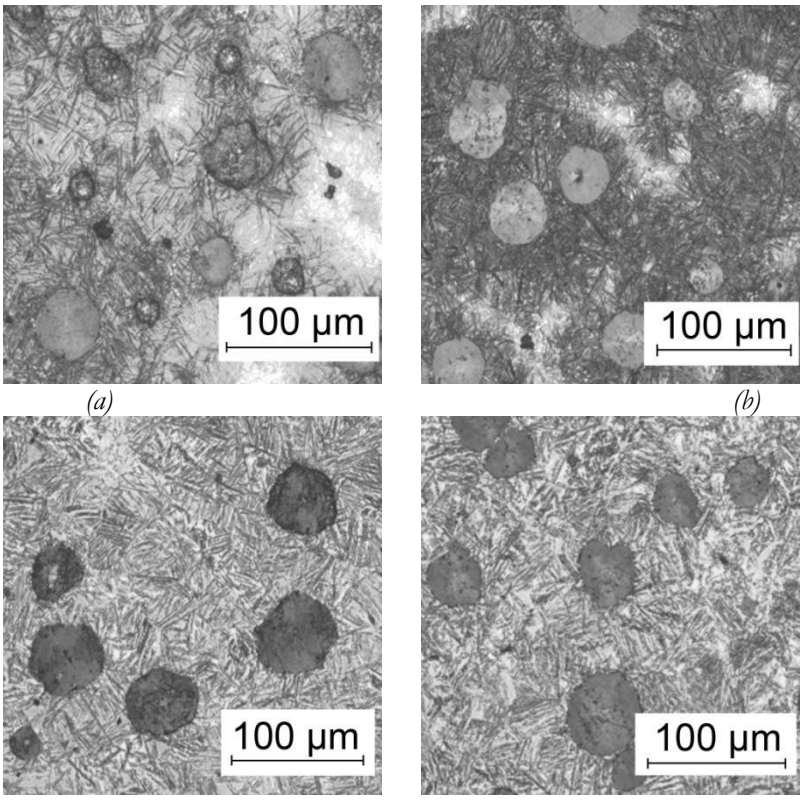

(a) *(b)*

(c) *(d)*

Figure 4: Microstructure of ADI-2 austempered at 523 K (250 °C) for (a) 30 minutes and (b) 3 hours, respectively 673 K (400 °C) for (c) 30 minutes and (d) 3 hours

B. Tensile Properties

1. Tensile properties of the as-cast materials

The 0.2% proof stress (PS), ultimate tensile strength (UTS) and the total elongation to fracture (TE) of the as-cast materials for ADI-1 and ADI-2 are shown in Table III. The data presented are the average values of three samples for each material.

Table III. Tensile Properties of the As-cast Materials

	PS [MPa]	**UTS [MPa]**	**TE [%]**
ADI-1	451	789	6.5
ADI-2	470	827	5.2

2. Influence of austempering temperature on tensile properties

For a specified austempering time, the tensile properties of the materials vary with the austempering temperature. It is noted that the proof strength and the ultimate tensile strength generally decreases as the austempering temperature increases. This is related to the previously described microstructural behavior of the materials for increasing austempering temperature. A higher austempering temperature results in coarser ferrite structure and an increased volume fraction austenite, which decreases the strength of the material but increases the ductility. The combination of high austempering temperature and long austempering time however leads to a significant decrease in total elongation due to the start of the second stage reaction. In the second stage reaction carbide is obtained, which makes the material brittle[6]. Figure 5 compares the stress-strain curves for ADI-1, as-cast and austempered at different temperatures for 1 hour.

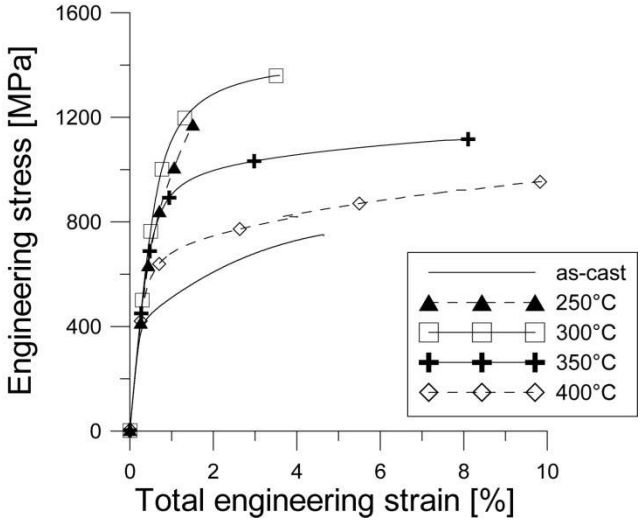

Figure 5: Tensile test curves of ADI-1 as-cast and austempered for 1h at different temperatures

3. Influence of austempering time on tensile properties

Figure 6 compares the stress-strain curves for ADI-1 as-cast and austempered at 623 K (350 °C) for different times. The influence of austempering time on the tensile properties of the materials for a specified austempering temperature is shown in Figure 7 (ADI-1) and Figure 8 (ADI-2). It is seen that for low austempering temperatures the austempering time greatly affects the proof strength and the ultimate tensile strength. As the austempering time increases, the strength increases while the total elongation decreases. For higher austempering temperatures, the effect of austempering time on the tensile strengths is significantly lower.

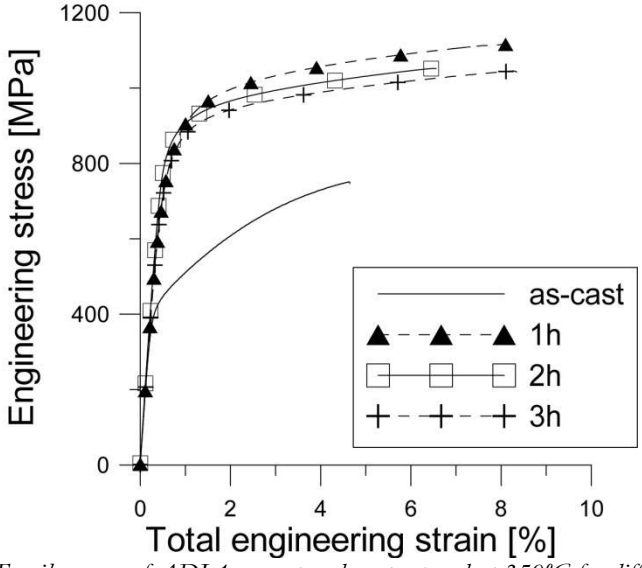

Figure 6: Tensile curves of ADI-1 as-cast and austempered at 350ºC for different times

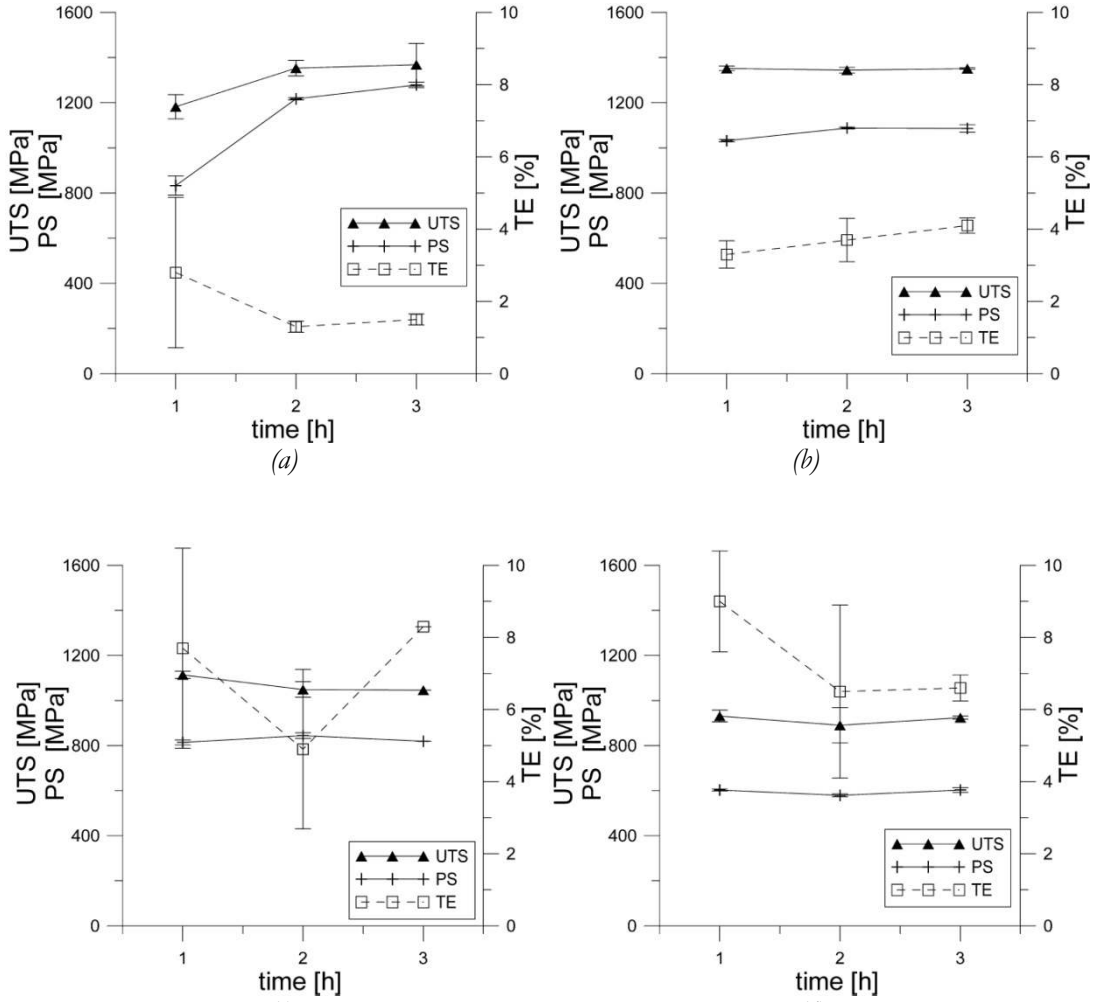

Figure 7: Influence of austempering time on the tensile properties of ADI-1 austempered at (a) 523 K (250 °C), (b) 573 K (300 °C), (c) 623 K (350 °C) respectively (d) 673 K (400 °C)

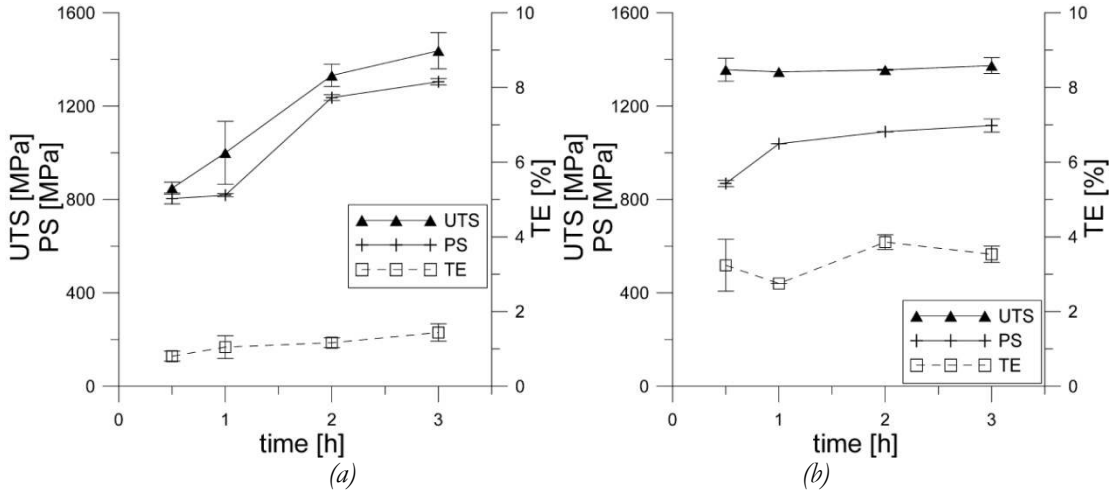

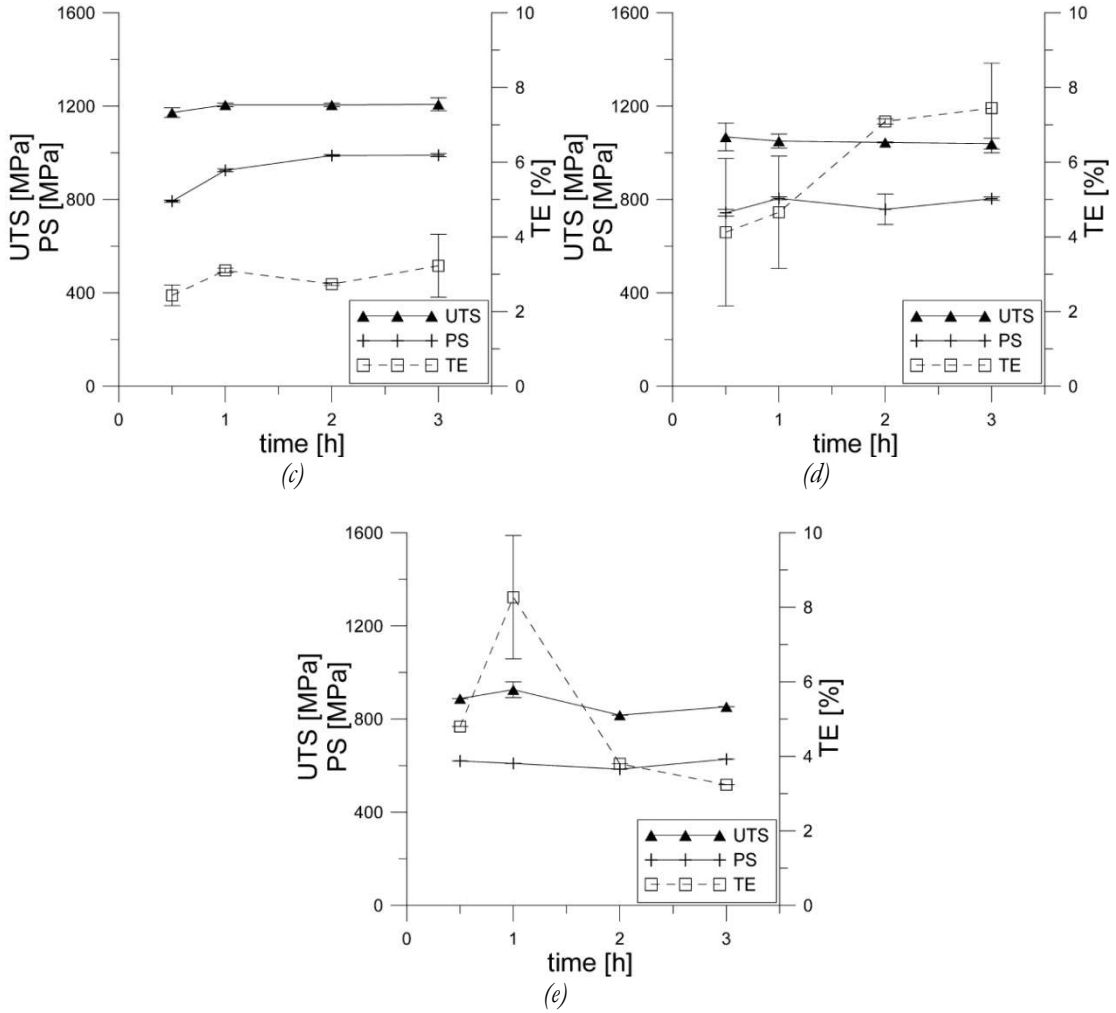

Figure 8: Influence of austempering time on the tensile properties of ADI-2 austempered at (a) 523 K (250 °C), (b) 573 K (300 °C), (c) 598 K (325 °C), (d) 623 K (350 °C) respectively (e) 673 K (400 °C)

C. Plastic Behavior

1. Influence of austempering temperature on the strain hardening exponent

Figure 9 shows the influence of austempering temperature on the strain hardening exponent for ADI-1 and ADI-2. It is noted that the strain hardening exponent initially decreases when the austempering increases. At a certain temperature it however reaches a minimum and thereafter starts to increase. This behavior can be explained by the previously described relationship between austempering temperature and the volume fractions of austenite and ferrite. Austenite is a FCC structure with a large number of slip planes that has a higher ductility and strain hardening rate than ferrite, which is a BCC structure[3]. When the austempering temperature is low the volume fraction ferrite is high and thus dominates the strain hardening behavior. The ferritic structure is very fine, but increasing the austempering temperature leads to a coarser ferritic structure and a decreasing volume fraction ferrite. This leads to fewer interface areas, and weaker interaction between dislocations and carbon atoms, which decreases the strain hardening exponent[8]. At a certain temperature, known as the critical austempering temperature[8], the volume fraction austenite has increased to the extent that the effect on the strain hardening exponent from the austenite dominates over the effect from the now decreased volume fraction ferrite. Thus the strain hardening exponent increases with increased temperature above the critical austempering temperature.

Note that at a low austempering temperature of 523 K (250 °C) combined with a short austempering time of 0.5-1h the strain hardening exponent is very high. This can be explained by the low diffusion rate of carbon at this austempering temperature[8], which may result in a large amount of unreacted metastable austenite and reacted metastable austenite after austenitizing. These types of austenite may form martensite when cooled or stressed[5]. Martensite is very hard and brittle, which leads to a higher value of the strain hardening exponent.

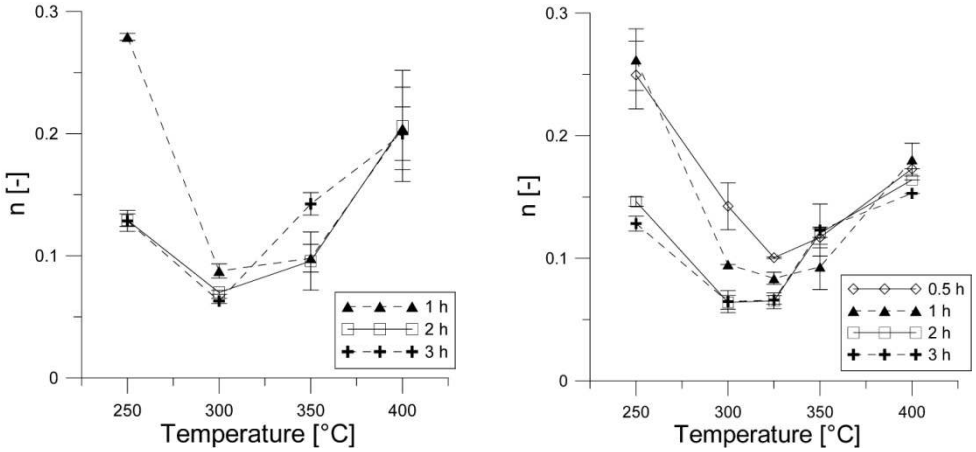

(a) *(b)*

Figure 9: Influence of austempering temperature on the strain hardening exponent for (a) ADI-1 (b) ADI-2

2. Influence of austempering time on the strain hardening exponent

The influence of austempering time on the strain hardening exponent is shown in Figure 10. For the lower austempering temperatures, 523-598 K (250-325 °C), it is noted that the strain hardening exponent decreases as the austempering time increases. An increased austempering time promotes growth of the ferrite needles[4], thus the contribution from ferrite on the strain hardening behavior increases and the strain hardening exponent decreases. It is also noted that at these low austempering temperatures there is a large difference in the strain hardening exponent between the austempering times of 1 and 2 hours, but a small difference between the times of 2 and 3 hours. This may be explained by the different carbon contents in the different types of austenite. At a low austempering temperature the carbon diffusion rate is low and the diffusion distances are short. This encourages new ferrite nucleation rather than ferrite growth. The new ferrite plates nucleate close to the existing ones which gives a fine structure[11]. The austenite close to the existing ferrite plates at the beginning of the austempering exists as reacted metastable austenite. The reacted metastable austenite is rather quickly transformed into reacted stable austenite because a relatively small increase in carbon content is needed. However when the ferrite growth reaches the unreacted metastable austenite, a larger increase in carbon content is needed to transform it into reacted stable austenite. This transformation thus needs a larger amount of carbon to diffuse, which requires a longer time. For the higher austempering temperatures the strain hardening exponent is more constant over time. At higher austempering temperature levels the diffusion rate of carbon is higher, thus a shorter time is needed to transform metastable austenite into stable austenite. At an austempering temperature of 573 K (300 °C) and an austempering time of 2-3 hours the lowest values of the strain hardening exponent are noted. Since ferrite has a lower strength coefficient than austenite[10], this indicates that the microstructure with the highest amount of ferrite and the lowest amount of austenite is obtained.

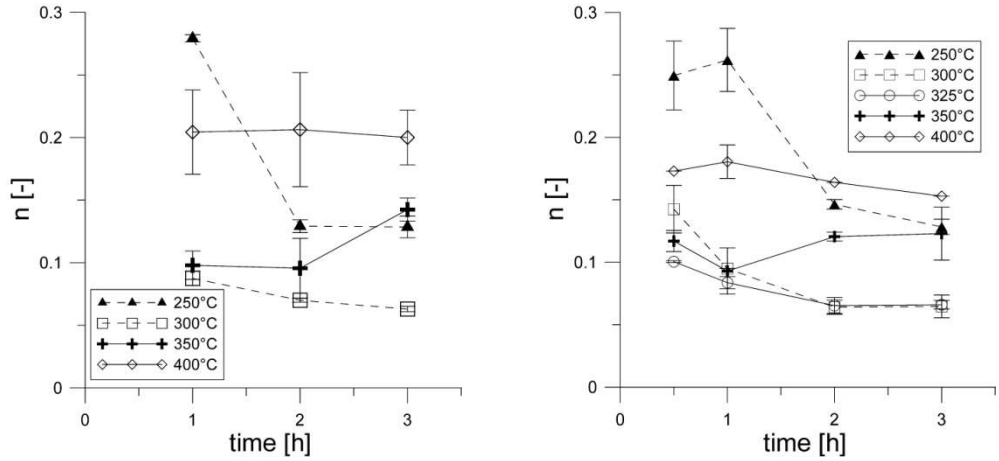

(a) *(b)*

Figure 10: Influence of austempering time on the strain hardening exponent for (a) ADI-1 (b) ADI-2

3. Influence of austempering temperature on the strength coefficient

Figure 11 shows the influence of the austempering temperature on the strength coefficient *K*. It is seen that the strength coefficient decreases as the austempering temperature increases. As previously discussed the ausferritic matrix becomes coarser as the austempering temperature increases, thus the strength of the material decreases. At an austempering temperature of 623 K (350 °C) it is however noted that the strength coefficient increases or reaches a plateau. This can be explained by rewriting Eq. [4] as Eq. [6].

$$K = \frac{\sigma}{(\varepsilon_{pl})^n} \qquad [6]$$

This clarifies that the strength coefficient is not only determined by the strength but also the strain and the strain hardening exponent *n*. The strain hardening exponent increases at austempering temperatures above 623 K (350 °C), which causes the denominator of Eq. [6] to decrease. Since the strain is raised to the power of the strain hardening exponent an increase in the strain hardening exponent has a larger effect on the strength coefficient than a decrease in strength and causes the strength coefficient to level out or even increase at austempering temperatures above 623 K (350 °C). This emphasizes that the strength coefficient is only an indication of the strength potential of the material, but to determine the actual strength it must be evaluated in combination with the strain hardening exponent.

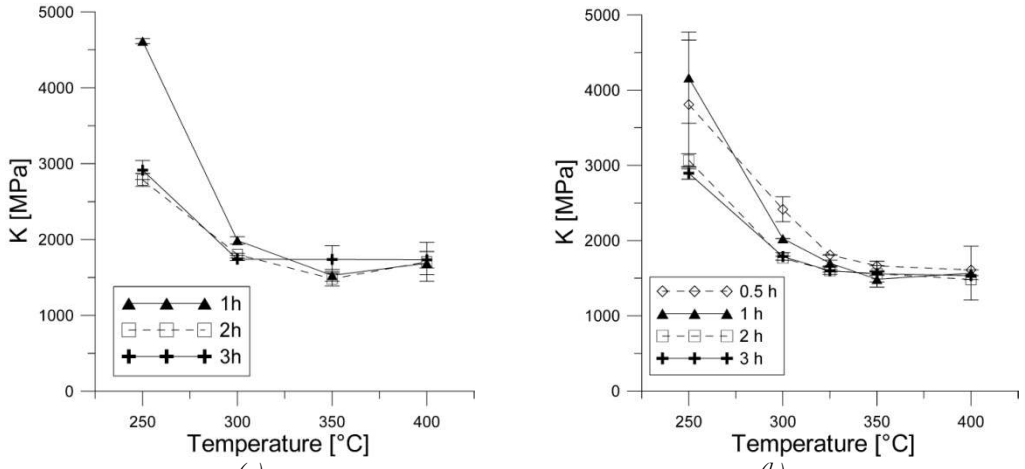

(a) *(b)*

Figure 11: Influence of austempering temperature on the strength coefficient for (a) ADI-1 (b) ADI-2

4. Influence of austempering time on the strength coefficient

Figure 12 shows the influence of austempering time on the strength coefficient. For a low austempering temperature of 523 K (250 °C) the strength coefficient has a high initial value which decreases with

increasing austempering time. This is seen in Figure 12, and can be explained by the microstructural behavior and the different types of austenite present. At a low austempering temperature and a short austempering time the amount of unreacted metastable austenite and reacted metastable austenite is high. Martensite may then form when the material is cooled or stressed, thus a high value of the strength coefficient is obtained[4]. As the austempering time increases, the amount of metastable austenite decreases which reduces the amount of martensite and thus decreases the strength coefficient. The same explanation that describes the time dependency of the strain hardening exponent at low austempering temperatures can thus be applied to the strength coefficient. For higher austempering temperatures the austenite stabilizes more quickly. The strength coefficient is hence more constant over time.

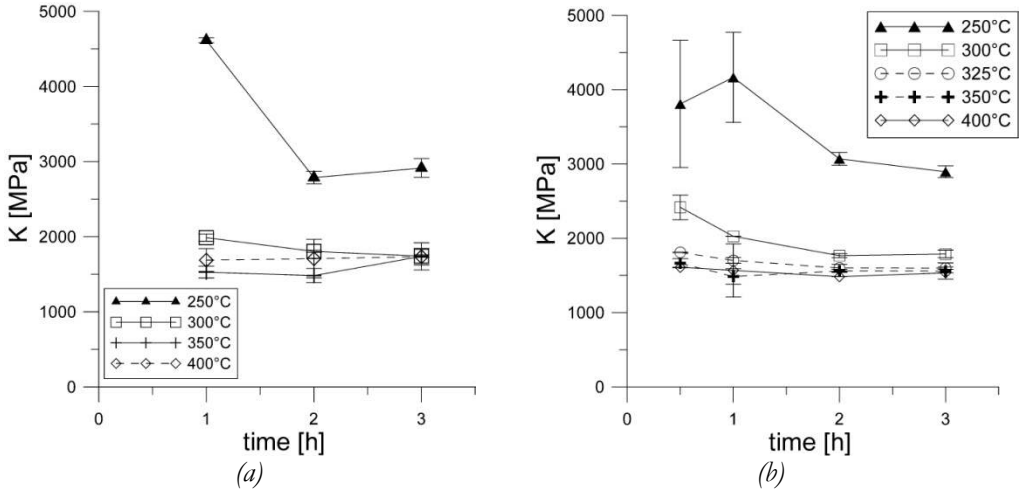

Figure 12: Influence of austempering time on the strength coefficient for (a) ADI-1 (b) ADI-2

IV. CONCLUSIONS

Austempering temperature and austempering time heavily affect the values of the strain hardening exponent and the strength coefficient as well as the tensile properties of ADI alloys. The following relations are observed:

- The value of the strain hardening exponent initially decreases as the austempering temperature increases, reaches a minimum at the critical austempering temperature and then increases.
- For low austempering temperatures the strain hardening exponent decreases as the austempering time is increased. For higher austempering temperatures the value is more constant.
- The strength coefficient decreases with increased austempering temperatures, but levels out at or increases after the critical austempering temperature.
- For low austempering temperatures the strength coefficient decreases with increased austempering time. At higher austempering temperatures the value is more constant.

These relations are explained by the microstructural behavior of ADI alloys during austempering. In terms of machining it is of interest to achieve a low value of the strain hardening exponent. The lowest value of the strain hardening exponent is for both alloys obtained using an austempering temperature of 573 K (300 °C) and an austempering time of 3 hours. These austempering parameters also result in a low value of the strength coefficient and high values of the tensile properties.

ACKNOWLEDGEMENTS

The authors would like to thank the Swedish Agency for Innovation Systems (VINNOVA) for financing the research project VI (Weight and volume Intelligent cast components) in which the present work has been performed.

REFERENCES

1. Y. Sahin, M. Erdogan and V. Kilicli, *Mater. Sci. Eng. A,* 2007, vol. 444, pp. 31-38.

2. P. P. Rao and S. K. Putatunda, *Mater. Sci. Eng. A,* 2003, vol. 349, pp. 136-149.

3. J. Zimba, D. J. Simbi and E. Navara, *Cem. Concr. Compos.,* 2003, vol. 25, pp. 643-649.

4. B. V. Kovacs, *AFS Trans.,* 1994, vol. 102, pp. 417-420.

5. J. L. Garin and R. L. Mannheim, *J. Mater. Process. Technol.,* 2003, vol. 143-144, pp. 347-351.

6. J. R. Davis, *ASM Handbook*, *vol. 4: Heat Treating*, 1st. ed., ASM International, Materials Park, OH, 1997, pp. 682-692.

7. S. K. Putatunda and P. K. Gadicherla, *Mater. Sci. Eng. A,* 1999, vol. 268, pp. 15-31.

8. J. Yang and S. K. Putatunda, *Mater. Sci. Eng. A,* 2004, vol. 382, pp. 265-279.

9. T. Sjögren and I. L. Svensson, *Metall. Mater. Trans. A,* 2007, vol. 38, pp. 840-847.

10. S. K. Putatunda, S. Kesani, R. Tackett and G. Lawes, *Mater. Sci. Eng. A,* 2006, vol. 435-436, pp. 112-122.

11. A. Trudel and M. Gagné, *Can. Metall. Q.,* 1997, vol. 36, pp. 289-298.